The published version of the paper "Marco Breccolotti, Santino Gentile, Mauro Tommasini, Annibale Luigi Materazzi, Massimo Federico Bonfigli, Bruno Pasqualini, Valerio Colone, Marco Gianesini, Beam-column joints in continuous RC frames: Comparison between cast-in-situ and precast solutions, Engineering Structures, Volume 127, 2016, Pages 129-144, ISSN 0141-0296 " is available at: https://doi.org/10.1016/j.engstruct.2016.08.018.

Beam-column joints in continuous RC frames: comparison between cast-in-situ and precast solutions

Marco Breccolotti[a,*], Santino Gentile[b], Mauro Tommasini[c], Annibale Luigi Materazzi[a], Massimo Federico Bonfigli[a], Bruno Pasqualini[b], Valerio Colone[b], Marco Gianesini[b],

[a] *Department of Civil and Environmental Engineering, Perugia, Italy*
[b] *Technip, Rome, Italy*
[c] *MOST Monitoring and Structural Testing, Rome, Italy*

Abstract

The use of precast reinforced concrete elements is rapidly increasing since this technique has several advantages over traditional cast-in-situ structural members such as lower manufacturing time and costs and a better quality control. Nevertheless, cast-in-situ solutions intrinsically allow building moment-resisting frames, a behavior that is usually hard to achieve using precast elements. In this paper a technical solution able to offer both high strength and ductility, simplicity of construction of the prefabricated elements and ease of assembly on site is presented. The solution realizes the continuity between beam and column by means of loop splices and cast-in-place concrete with steel fibers to improve the ductility of the concrete struts

*Corresponding author
Email addresses: brec@unipg.it (Marco Breccolotti), sgentile@technip.com (Santino Gentile), tom@mostsrl.eu (Mauro Tommasini), annibale.materazzi@unipg.it (Annibale Luigi Materazzi), federico.bonfigli@strutture.unipg.it (Massimo Federico Bonfigli), bpasqualini@technip.com (Bruno Pasqualini), vcolone@technip.com (Valerio Colone), mgianesini@technip.com (Marco Gianesini)

in the wet joint. The connection has been experimentally tested and compared to an analogous cast-in-situ one. The experimental results confirmed its good structural performances in terms of strength and ductility. Numerical investigations tuned on the basis of the experimental results allowed the improvement of the design to achieve reduced column damages for higher drift values while maintaining practically unchanged structural performances.
Keywords: Earthquake resistant structures, Precast structures, Beam-column joints, Experimental tests, FE Modeling

1. Introduction

Precast reinforced concrete techniques are increasingly replacing the cast-in-situ reinforced concrete solutions. This can be ascribed to the remarkable advantages that the prefabrication offers against traditional techniques such as the better quality of the components made in the workshop, the lower manufacturing costs, the possibility of realizing the precast components even in adverse weather conditions and the speed of construction. The cast-in-situ structures possess, however, the advantage of providing continuous frames intrinsically resistant to bending moment. This behavior should, instead, be specifically created in the prefabricated structures. Hence the choice of the right technology for the precast system is of major importance and the aim, for the designer, is to obtain a solution that is capable of obtaining the required performances in terms of load bearing capacity and ductility while minimizing construction manpower, time and costs. A number of technical solutions have been proposed for this purpose in the past, mainly focusing the attention on the load bearing capacity of the connection system. This study presents a technical solution able to offer both high strength and ductility in the plastic range, simplicity of construction of the prefabricated elements and ease of assembly on site. The comparison of cyclic tests with imposed displacements up to a drift ratio of 3.5% on a couple of external beam-column joints allowed verifying the structural behavior of the prefabricated solution. The results of the experimental tests showed a seismic performance of the prefabricated joint very similar to that of the 'twin' cast-in-place joint. A sophisticated arrangement of sensors has also allowed to analyze in detail the behavior of both technological solutions. Finally, FE analyses tuned on the results of the experimental tests have been used to improve the design of the precast joint moving the critical region outside the connection zone without reducing stiffness, strength and ductility of the joint.

2. Literature review on beam-column joint in precast structures

The first researches on beam-column joints have been carried out, obviously, with reference to cast-in-situ joints.

Paulay et al. [1] were among the firsts to investigate the behavior of interior beam-column joints under seismic actions. They highlighted the existence of two shear resisting mechanisms, one involving joint shear reinforcement and the other the concrete strut. Based on extensive experimental results carried out in more than 15 years, Paulay [2] demonstrated the disposition of internal forces with diffuse diagonal cracking of the concrete core and that joint shear reinforcement is necessary to sustain a diagonal compression field rather than providing confinement to the compressed concrete in the joint core.

Later on, similar research efforts have been provided also for precast structures. In this case the importance of connection detailing for structures subjected to severe seismic action emerged since the beginning of the 90's and different technical solutions have been proposed for the beam-column joints.

A wide joint research project called PRESSS was carried out by researchers from the United States and Japan on the seismic design and performance of precast concrete structural systems [3]. The objectives of this program were the development of effective seismic structural systems for precast buildings and the preparation of seismic design recommendations for incorporation in the building codes. The attention of U.S. researchers was focused on ductile connections capable of protecting the precast elements against inelastic deformations by means of a capacity design while the Japanese program was concentrated on the strong-connection approach. The results of the research project were pointed out by Priestley et al. [4].

Restrepo et al. [5] tested six types of subassemblages of moment resisting frames located at the perimeter of buildings. Connections between the prefabricated elements were realized at beam midspan or at the beam-to-column joint region with cast-in-place concrete. The experimental results showed that the connection details can be successfully designed and constructed to emulate cast-in-place construction.

Priestley and MacRae [6] tested two ungrouted post-tensioned, precast concrete beam-column joint subassemblages under cyclic reversals of inelastic displacements to determine their seismic response. The test units were designed with greatly reduced beam and joint shear reinforcement compared with equivalent monolithic joints, but implementing a special spiral confinement of the beam plastic hinge regions. Both subassemblages performed well, with only minor cosmetic damage being recorded up to drift ratios of 3% or more. Energy absorption of the hysteretic response, though small, was larger than expected. A very low residual drift was observed after a severe earthquake. This is a characteristic of the unbonded prestressing system and is a significant advantage over conventional cast-in-place reinforced concrete construction, where very high residual drifts generally occur. It was concluded that satisfactory seismic performance can be expected from well-designed ungrouted precast, post-tensioned concrete frames.

Two full-scale beam-to-column connections of a precast concrete frame were designed, following the strong-column weak-beam concept, and tested by Alcocer et al. [7] under uni-directional and bi-directional cyclic loading. Conventional mild steel reinforcing bars, rather than welding or special bolts, were used to achieve beam continuity. Test results showed that the performance of both beam-column connections was roughly 80% of that expected from monolithic reinforced concrete constructions with a ductile behavior due to hoop yielding. Bar pullout and strength values were nearly constant up to drifts of 3.5%.

Korkmaz and Tankut [8] tested six 1/2.5 scaled beam-beam connection subassemblies under reversed cyclic loading. The first specimen was a monolithic one used as reference. The others were precast specimens composed of a middle precast beam placed between two cantilever beams connected to the columns. The connection between the precast elements region was obtained by lap splicing of the top reinforcement and welding between the steel plates anchored to the bottom of the middle and cantilever beams. Cast-in-situ concrete on the top of the beams completed the connection. The results of the tests allowed recognizing that this connection detail was not suitable for seismic use. Proper modifications to obtain significant performance improvements have been subsequently proposed and tested by the Authors.

A similar solution has been proposed also by Ong et al. [9] who used the DfD (Design for Disassembly) method to increase material reusability in the construction industry, allowing the reuse of the structural components after the decommissioning of the structure instead of their demolition and recycling of the resulting debris. Parastesh et al. [10] tested a new ductile moment-resisting beam-column connection capable of providing good structural integrity in the connections and reduced construction time. Their solution eliminated the need for formworks and welding and minimized cast-in-place concrete volume by realizing a discontinuity in the column filled by the cast-in-situ concrete.

A wide research project, SAFECAST [11, 12], has been recently completed by the Joint Research Center of the European Commission. In this project a full-scale three-storey precast building was subjected to a series of pseudodynamic tests to evaluate the behaviour of various parameters like the types of mechanical connections (traditional as well as innovative) and the presence or absence of shear walls along with the framed structure.

2.1. Classification of precast beam-column connections

Nowadays connections between precast beams and columns can be separated into three main classes: dry, hybrid and wet connections.

The mechanical connections made with steel elements and bolts belong to the dry class. Among these connections are those tested by Vidjeapriya and

Jaya [13]. The Authors carried out tests on two types of simple mechanical 1/3 scale concrete beam-column connections realized with cleat angle with 1 or 2 stiffeners, subjected to reverse cyclic loading. The results of the tests were then compared with the performance of a reference monolithic beam-column connection. The Authors observed that ultimate load-carrying capacity of the monolithic specimen was superior to that of both precast specimens, while satisfactory behavior of the latter was found in terms of energy dissipation and ductility.

Hybrid connections are those where mechanical connections and cast in situ concrete are used at the same time. Hybrid connections have been tested by Choi et al. [14], Ong et al. [9]. Sometimes with the same term has been indicated a combination of mild steel and post-tensioning steel where the mild steel was used to dissipate energy by yielding and the post-tensioning steel was used to provide the shear resistance through friction developed at the beam-column joint [15].

Wet connections are generally made up of rebar splices and cast-in-situ concrete. Among the different types of rebar splices, very good mechanical properties have been shown by loop splice connections. Several studies showed that the mechanical behaviour of this type of joint, if properly designed, can be considered similar to that of ordinary RC elements [16, 17]. Moreover, the use of loop splice is also frequently used in practice to establish continuity between precast deck elements in steel-concrete composite bridges [18].

Since the beginning it was recognized the usefulness of steel fibers to develop ductile moment resisting wet connections designed to act as a plastic hinge during earthquakes [19]. High performance fiber reinforced cement composite (HPFRC) matrix was used to develop a high energy absorbing joint for precast/prestressed concrete structures in seismic zones reducing the amount of transverse reinforcement in the connection by using steel fibers in the connection matrix [20]. Ultra high performance fiber reinforced concretes (UHPFRC) were also used in conjunction with short reinforcement splice lengths to develop continuity connections between precast elements to achieve a safe construction process, reduced construction time and avoid the use of complex reinforcing details, while maintaining high quality level [21].

3. Proposed wet joint for beam-column connection

The wet joint between precast beams and columns presented in this study has been developed as a standard solution for pipe rack structures, commonly used within worldwide oil and gas plants but it could be also adopted in other continuous precast RC frames. The standard cast-in-situ solution has been designed according to the ACI 318 code [22]. An example of the pipe rack structures is shown in Fig. 1. They are generally composed of transversal frames that are repeated along the path of the piping lines at a given spacing. Considering the significant heights that can be reached by such structures is clear the importance of having in seismic-prone regions a moment resisting frame, especially in the transversal direction. The construction of such facilities, which are very often located in remote regions, could turn out to be far too complicated with the traditional cast-in-situ technique. A precast solution would instead allow a much easier building process with reduced construction time and costs.

Assuming initially a cast-in-situ frame, the demand of the beam critical section at the beam-column intersection has been evaluated as $M_u = 1100$ kNm. By taking into account the capacity reduction factor for tension controlled failure $\phi = 0.9$, the rectangular beam section 500 mm wide and 900 mm tall has been reinforced with 4 bars of 28 mm diameter and 2 bars with 25 mm diameter placed in the upper and lower sides. The nominal bending strength of this section is equal to $M_n = 1233$ kNm.

A wide variety of solutions for precast concrete pipe racks has been developed along the years. All of them aimed at obtaining a monolithic frame from precast pieces. Three big families of solutions can be identified:

- Cast-in-situ joints between precast beams and columns;
- Mechanical connectors between precast beams and columns;
- Monolithic precast frames.

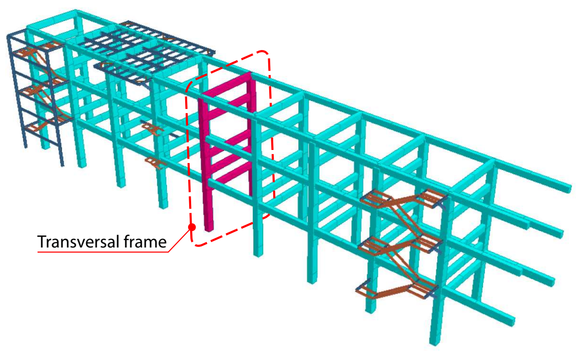

Figure 1: Example of pipe rack for oil and gas plants.

For the structure under study an innovative kind of cast-in-situ joint which limits the cast-in-situ volume to a minimum amount, without connectors, scaffolding, formworks and extra material has been designed and developed. In the proposed construction technique the transversal frames are made up of two precast concrete columns connected with several beams at different heights (Fig. 2). Each beam hosts specific elements (pipes, maintenance platforms, ...) functional to the developing plant.

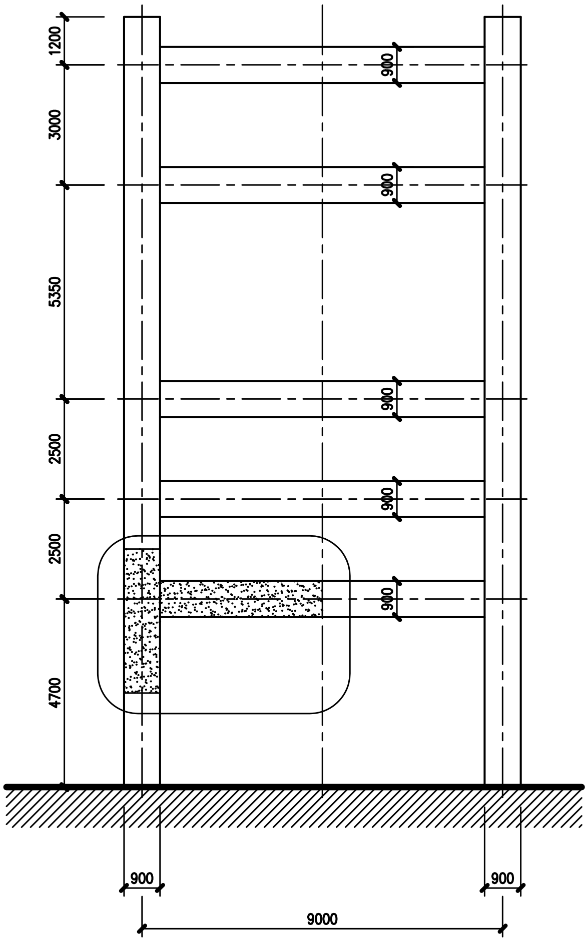

Figure 2: Full-scale RC structure for pipe racks (dimensions in mm). The beam-column connection realized in 1:3 scale for the experimental tests is highlighted.

Fiber reinforced concrete (FRC) has been chosen to realize the wet connection between the precast beams and columns for its favorable properties, both in tension as in compression. The protruding rebars from column and beams that will be embedded in the FRC casts are shown in Fig. 3. At the beam ends the cross section of the prefabricated beam is gradually enlarged, and thereafter divided into two prismatic elements with rectangular section, called shoulders, which define a containment, the formworks, for the next cast-in-situ.

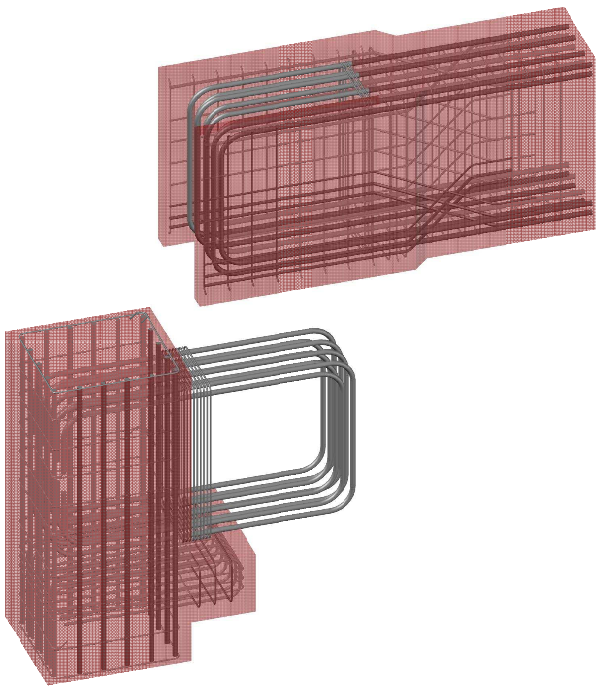

Figure 3: Protruding rebars from column and beam for the wet joint connection.

Special attention has been paid during the design process to the strength and ductility aspects but also to the ease of installation. The analyses of stresses and forces inside the column joint and on the hooked rebars have been carried out using well established design procedures [23, 24].

The assembly process and completion is shown in Fig. 4. In phase 1 the full height precast columns are erected. They are provided with bolted brackets that will subsequently bear the precast beams. In this phase are also visible the steel rebars that protrude from the column and from the beam. They will be later incorporated in the final casting. In phase 2 the precast beams are leaned on the brackets by means of the 2 lateral RC shoulders. This is possible thanks to the shape of the solution that allows the launch of the beam from above. In phase 3 the closed stirrups that were already placed around the rebars protruding from the columns and the beams are disposed with the correct spacing. In the final phase the connection is completed by pouring the FRC in the joint using the lateral shoulders as formwork.

4. Experimental program

To compare the precast solution with the corresponding cast-in-situ construction, an experimental program was carried out. Two reduced scale models, the cast-in-situ reference model and the corresponding precast solution, have been designed and built. The test modules, i.e. the laboratory specimens representing the characteristics of a typical configuration of intersecting beams and columns, have been defined according to the provision of the relevant ACI standards [25, 26] for the most stressed connection of the moment frame shown in Fig. 2.

4.1. The specimens

Both the cast-in-situ and the precast joints were realized in a 1:3 scale. The adoption of this reduced scale is specifically allowed by the abovemen-

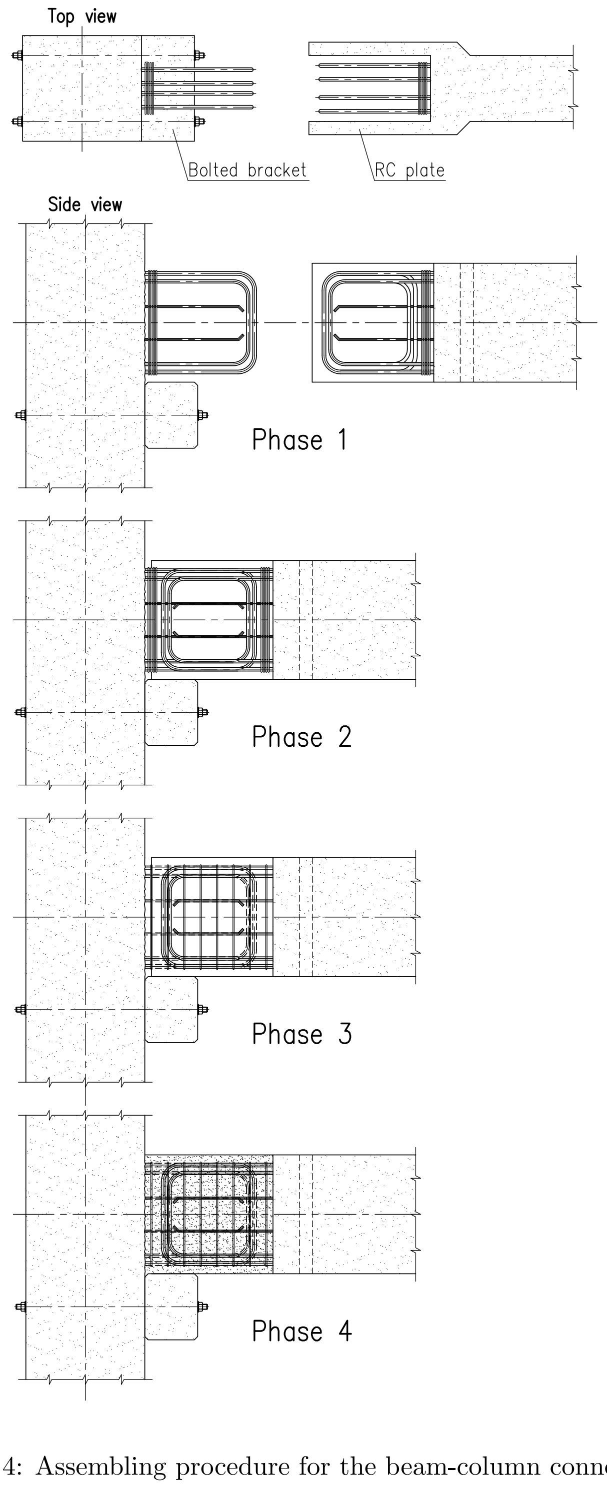

Figure 4: Assembling procedure for the beam-column connection.

tioned ACI standards. It has been thus assumed that no significant size effects with respect to the unscaled elements are expected. The bending and shear strengths of the beam critical section have been evaluated according to the ACI 318 code. Their values, neglecting the strength reduction factors, turned out to be $M_{n,red} = 47.2$ kNm and $V_{n,red} = 106.8$ kN. There is no risk of brittle shear failure in the beam since the shear value corresponding to the attainment of $M_{n,red}$, equal to 35.0 kN, is far below the shear strength $V_{n,red}$. It can also be observed that the scaling procedure turned out to provide a nominal bending strength $M_{n,red}$ of the scaled specimen that is very close to the scaled nominal bending strength $M_n/3^3 = 45.7$ kNm.

The geometry of the cast-in-situ joint and the reinforcement details are shown in Fig. 5. The beam section was 166.7 mm wide and 300 mm deep and its longitudinal steel reinforcement consist in 2 ϕ 12 mm and 1 ϕ 14 mm both in the upper and in the lower parts. The reinforcement ratio is thus approximately equal to 0.8%. The 14 mm central bars are eccentric with respect to the cross section axis to avoid the interference with the central bars of the column. Two ϕ 8 mm bars have been located in the center of the lateral sides of the section in order to better restraint the stirrups. These latter consisted in ϕ 6 mm bars with a spacing of 110 mm near the hinged connections and the joint, and with a spacing of 250 mm in the central portion where the shear forces are lower. The column had a cross-section 266.7 mm wide and 300 mm deep and its reinforcement is made up of 4 ϕ 16 mm along the edges of the section and 4 ϕ 14 mm in the middle of the sides. The stirrups had a spacing of 60 mm near the hinged connections where a concentrated load is applied, while in the remaining parts the spacing is

Concrete	Cement (kg/m^3)	W/C ratio	Sand (kg/m^3)	Gravel (kg/m^3)	Hyperplasticizer (l/m^3)	Fibers (kg/m^3)
Cast in situ	380	0.395	940	850	3.8	0
Precast	380	0.395	940	850	4.2	0
FRC	640	0.300	583	800	6.4	39

Table 1: Concrete mix designs used for the tested specimens.

approximately equal to 243 mm. Additional bars were located around the connection points between the RC elements and the mockup structure in order to prevent a local collapse of the sample outside the area of the joint connection. The precast joint has the same geometry and reinforcement of the cast-in-situ one, except for the area where the connection between the beam and the column is realized (see Fig. 6). Here the beam widened up to 233.3 mm, realizing an U-shaped connection that was supported by the RC bracket bolted to the column. This wider dimension does not affect the bearing capacity of the beam in the critical zone since the lateral thin concrete panels only serve as formworks for the FRC cast and there is no significant transfer of forces between these elements. Furthermore, as visible in the upper view of Fig. 6, a 17 mm gap prevents any contact between the lateral thin concrete panels and the column. The gap has been filled with deformable caulk prior to the casting of the FRC to avoid the transmission of significant stresses to the lateral RC brackets. Longitudinal ring-shaped bars come out from the beam and from the column in this region. When the placement of the beam on the bracket was completed, the continuity between the two elements was realized by means of a FRC cast that filled the U slot.

Three different types of concretes, two for the cast-in-situ and precast RC elements and one for the wet connection, have been used for the con-

Concrete	**Compressive**	**strength**
	53 hours	125 days
	(MPa)	(MPa)
Cast in situ	8.6	39.2
Precast	6.4	35.8
FRC	17.0	69.4

Table 2: Concrete compressive strength of the tested specimens.

Diameter ϕ (mm)	**Yielding stress** (MPa)	**Tensile strength** (MPa)	**Yielding strain** $(\mu\epsilon)$
6		443	
12	453	584	2199
14	466	602	2262

Table 3: Mechanical properties of the reinforcing steels.

struction of the test modules. Steel fiber reinforced concrete has been chosen for the concrete of the wet-joint to increase the ductility properties of the compressed strut in the connection. The mix designs of the three concretes are shown in Tab. 1 while the compressive strengths at 53 hours and at 125 days of the same mixes are listed in Tab. 2. The concrete compressive strength of the cast-in-situ, precast and steel fiber reinforced concretes at 125 days have been evaluated a few days before the testing of the two specimens. In the tables it can be noticed that the concretes used for the cast-in-situ and the precast elements have almost the same composition and achieved approximately the same compressive strength. The volume fraction of the fiber has been chosen taking into account the specific feature of the proposed connection. Obviously, the higher is the fiber content, the higher is the increase in strength and ductility but, on the other hand, high fiber content can lead to a significant reduction in the concrete workability. For the proposed beam-column connection the tensile strength and ductility of

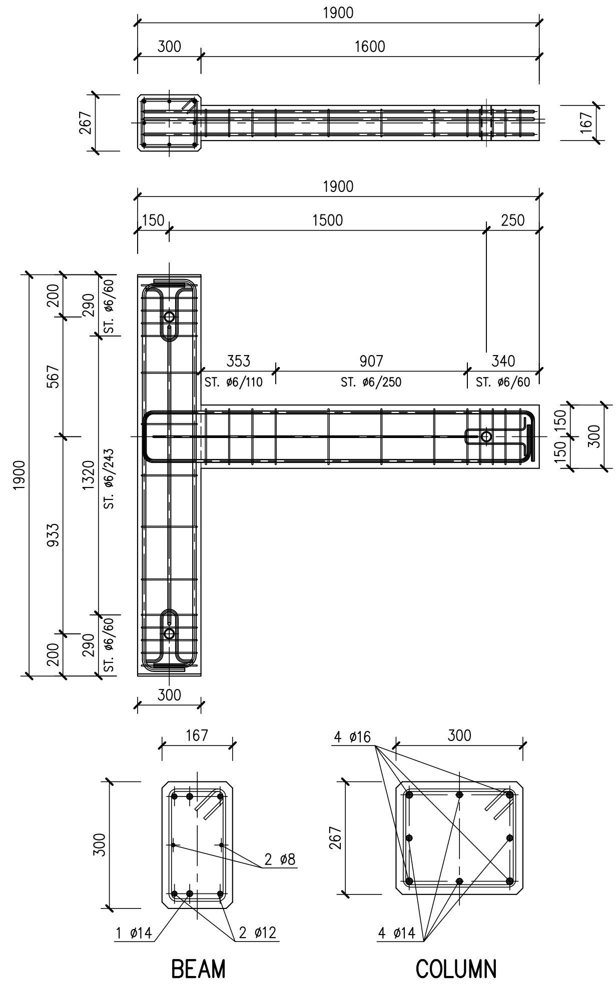

Figure 5: Geometrical dimension (mm) and reinforcement layout of the cast-in-situ specimen. Upper view, side view and cross-sections.

the cast-in-place concrete do not play a major role. In fact, at the interface between the cast-in-place concrete and the precast elements only a weak tensile strength (adhesion) can develop and, thus, in these regions cracks are primarily expected to occur. For this reason no significant increases in the tensile strength and in the toughness are necessary for the cast-in-situ

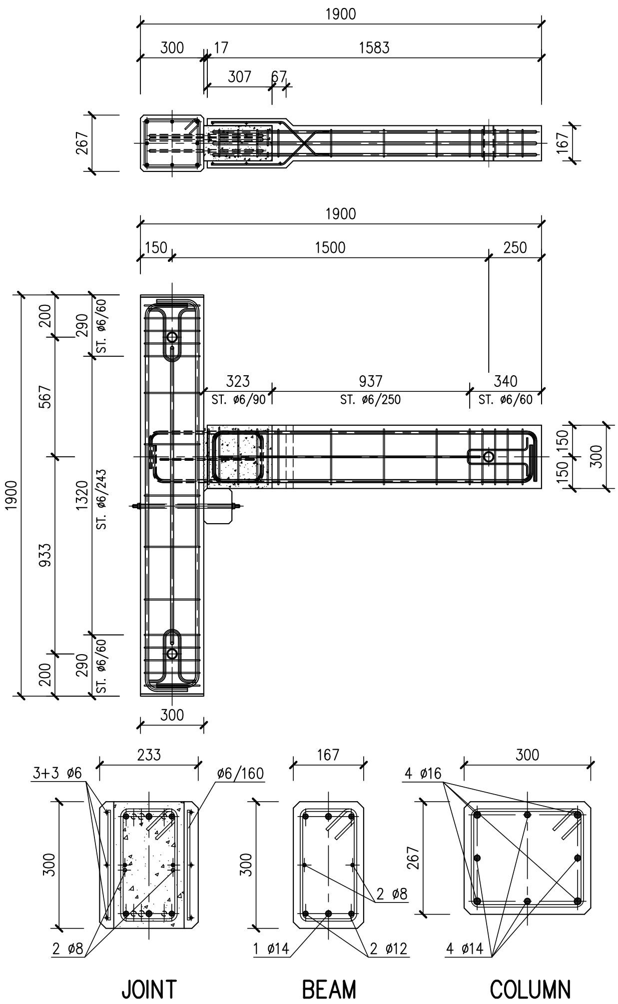

Figure 6: Geometrical dimensions (mm) and reinforcement layout of the precast specimen. Upper view, side view and cross-sections.

concrete. Conversely, good strength and good ductility properties are required for the compression stress-strain relationship in order to improve the behavior of the concrete strut inside the connection region. Considering the above mentioned reduction in the concrete workability and considering also the data reported in the works by Taerwe and Van Gysel [27], Neves and

Fernandes de Almeida [28] and Marar et al. [29], a fiber volume fraction of 0.5% has been judged suitable for the cast-in-place concrete. Among the different types of fibers, the steel ones have been selected for their ability to improve the flexural toughness and for their flexural fatigue endurance [30]. Commercially available steel fibers were used in the FRC. They are characterized by a length of 33 mm, a diameter of 0.55 mm, a tensile strength higher than 1200 MPa and double-end hooks to ensure a proper anchorage in the concrete. The content of fibers in the FRC was equal to 39 kg/m^3, resulting in a volumetric fraction approximately equal to 0.5%. B450C steel rebars have been used for every reinforcement. The mechanical properties of the steel rebars are listed in the Table 3.

Fig. 7 shows the reinforcement and the formwork of the cast-in-situ solution just before the concreting, whereas Fig. 8 shows the precast column just after the concreting.

4.2. Test setup

In order to correctly execute the experimental tests, an ad-hoc setup was designed (Fig. 9) and built (Fig. 10). The whole apparatus was installed inside a test chamber, delimited by a RC reaction wall. The column was supported by a steel cylinder whose function was that of providing the vertical reaction force without notable horizontal components. The horizontal reaction was instead provided by a stiff steel frame anchored on one side to the rigid RC wall, and on the other side to the lower part of the column using a pinned connection, thus allowing rotation to occur. On the upper part of the column an hydraulic jack attached to the reaction wall was connected to the column using a pinned connection. The jack provided the horizontal

Figure 7: Reinforcement and formwork of the cast-in-situ specimen.

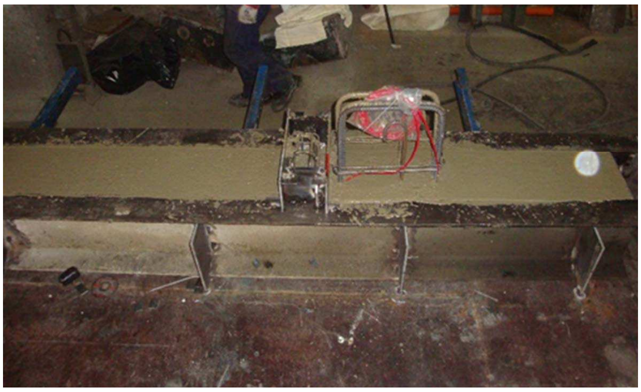

Figure 8: Precast column just after the concreting.

force that was used to control the column drift. The beam was connected by means of a pinned restraint to a steel frame. This latter was linked to a rigid steel base that was integral with the floor using a bolted connection. The steel frame applied a restraint to the beam only in the vertical direction allowing at the same time the horizontal movement of the beam itself (see Fig. 9). No notable horizontal restraining force was thus applied to the end of the beam. A second hydraulic ram actuator placed on the top of the column was used to apply a suitable compressive force to the column. The value of this force corresponds to the axial load induced in the column by the permanent loads in the overlying portion of the structure of the pipe rack (see Fig. 2) reduced by a scale factor of 9 to take into account the scale of the specimen. The reaction exerted by the jack was transmitted to the ground by means of two threaded steel rods.

This hydraulic jack was actuated by a manually operated hydraulic pump to impose the predetermined compressive force. In order to minimize the variations in trim during the execution of the tests, it was used a hemispherical head interposed between the vertical actuator and the top of the column. A load cell was installed between the actuator and the column to control and store the time history of the vertical load.

4.3. Sensors

The relative horizontal displacement between the bottom hinge and the top hinge of the column was monitored by means of two displacement sensors (Fig. 9): a wire transducer (WT) linked to the ground was applied on the top of the column at the same height of the hydraulic jack, while a linear variable displacement transducer (LVDT) was applied on the bottom hinge.

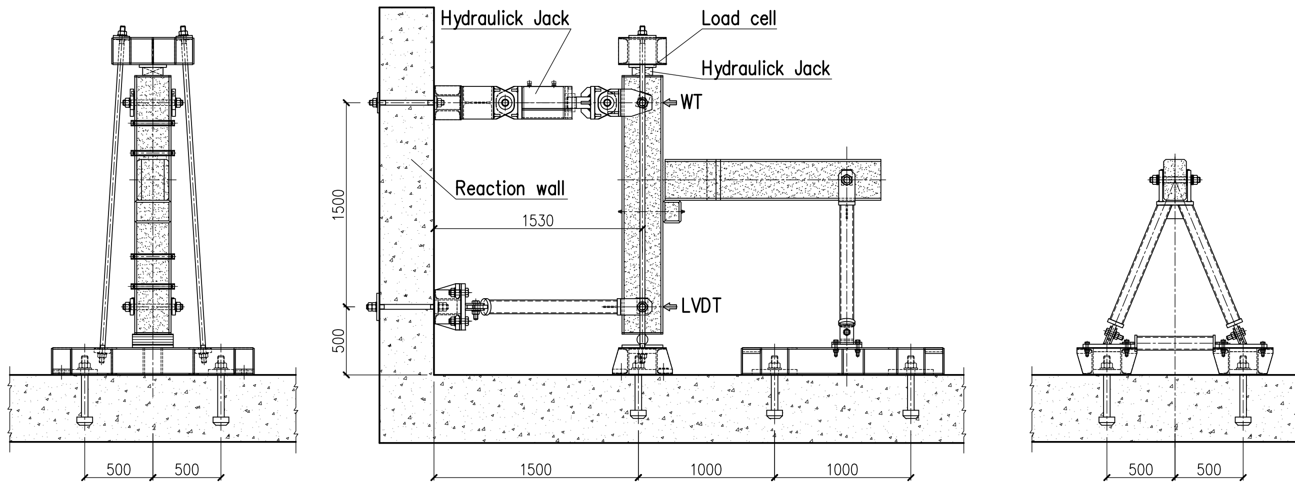

Figure 9: Schematic representation of the experimental test setup: rear view (left), side view (center) and front view (right).

Figure 10: Picture of the experimental setup before the beginning of precast joint test.

The difference between the two values defines the actual applied drift. A pressure transducer was used to measure the pressure in the hydraulic jack. Several sensors, shown in Fig. 11, were also applied to the experimental setup to monitor the joint behavior and to obtain a careful evaluation of the stresses in the concrete and in the reinforcing steel. Vibrating wire strain gauges (VWSG) were embedded into the concrete in the upper and in the lower areas of the beam section nearby the joint, both in the cast-in-situ and in the precast joint. The sensors have been placed just outside the critical region to avoid any drawback during the execution of the tests. Similarly, VWSGs were also fixed to the lower and upper steel bars of the beam (Fig. 12a). In addition, further VWSGs were also fixed in the precast joint to the steel rebars inside the column (Fig. 12b) to verify the actual transmission of stress from the reinforcing bars of the beam to those integral with the precast column. The choice of the vibrating wire strain sensors (compared to resistive strain gauges) has been made mainly considering the need of measuring the deformation of the concrete over a significantly long distance, compared to the size of the aggregates.

Additional potentiometric linear variable displacement transducers (PDT) were also applied to the joint to measure its overall deformation. One transducer was located on the upper part of beam section to detect the horizontal relative displacements between the upper outer layer of concrete and the outer concrete of the column. Similarly, another transducer was applied on the bottom part of the beam section. Finally two transducers were placed in a X-shaped configuration connecting the lateral concrete surface of the beam and the lateral surface of the column. The combination of the data coming from the two couples of PDT, each composed by one inclined PDT and by the opposite horizontal one, allowed verifying the shear deformation occurred in the beam critical zone during the tests that proved to be negligible. Sig-

Instrument	**Measure**	**Type**
Embedment vibrating wire strain gauges VWGSe	Concrete strain	GV-4200: 150 mm gauge length, 3000 μstrain ($\pm$1500), Linearity $<$ 0.5%, Internal thermistor (-20/+80 C)
Arc weldable vibrating wire strain gauges - VWGSaw	Rebar strain	GV-4200AW:150 mm gauge length, 3300 μstrain, Linearity $<$ 0.5%, Internal thermistor (-30/+80 C)
Linear variable potentiometric displacement transducers - PDT	Displacement between column and beam	Gefran PZ34-A-150: 150 mm range, Linearity 0.05%, Power supply: 12 Vcc
Linear variable differential transformer displacement transducers - LVDT	Displacement between ground and bottom of the column	HBM WA: 100 mm range, Linearity $\pm$0.01%, Power supply: 12 Vcc
Wire rotative potentiometric displacement transducers - WT	Displacement between ground and top of the column	Celesco PT101-0020-111-5110: 500 mm range, Linearity 0.07%, Power supply: 12 Vcc

Table 4: Instruments installed on specimens.

nals from the sensors were recorded using a double system of measurement based on two data acquisition units synchronized together by a digital line and configured for a scan data rate of 1 Hz.

4.4. Testing procedure

Joint specimens were subjected to a sequence of displacement-controlled cycles representative of the drifts expected under earthquake motions and defined in accordance to the ACI standards [25, 26]. The drift sequence, shown in Fig. 13, has been established complying with the following rules:

- the initial drift ratio must be within the essentially linear elastic response range;
- subsequent drift ratios must be not less than one and one-quarter times, and not more than one and one-half times the previous drift ratio;

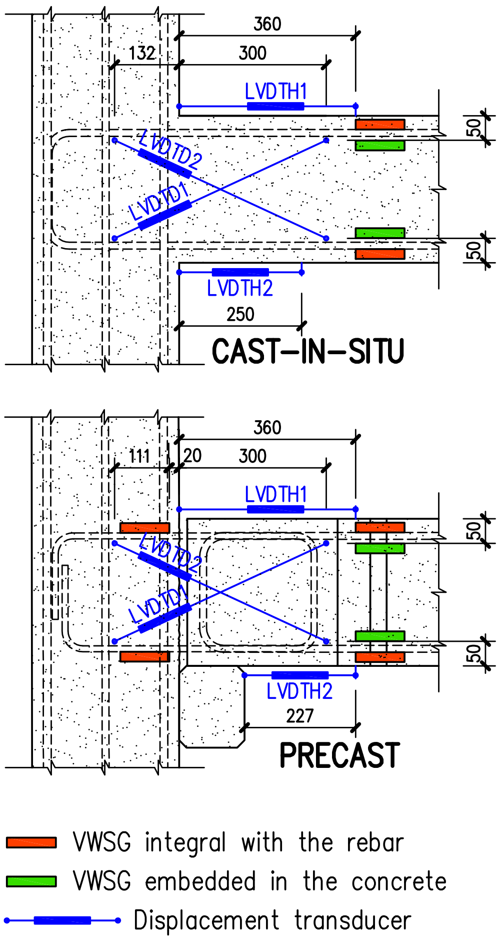

Figure 11: Schematic representation of the sensors.

- three fully reversed cycles must be applied for each drift ratio value.

Testing have been continued with gradually increasing drift ratio until it reached a value of 4.33%.

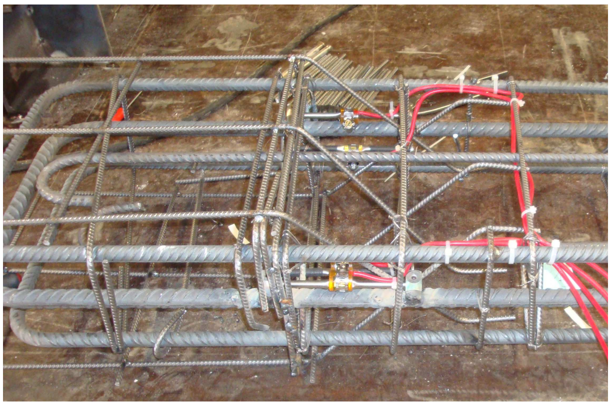

(a)

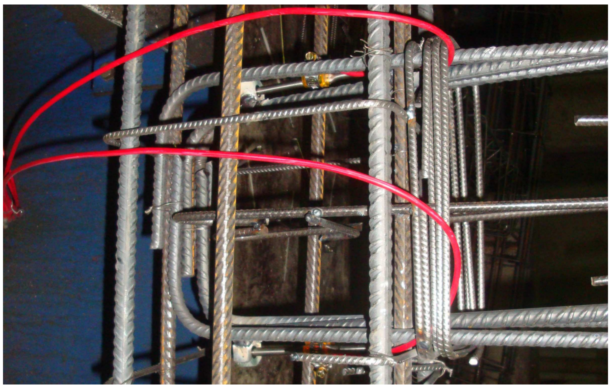

(b)

Figure 12: VWSGs fixed to the reinforcing steel: (a) in the precast beam and (b) to the reinforcing steel in the precast column.

5. Tests results

In the present chapter are presented and analyzed the results of the experimental investigations on the cast-in-situ and precast specimens. Being the objective of this study that of verifying if the precast joint fulfilled the provision of ACI Standards, the tests have been terminated after completing

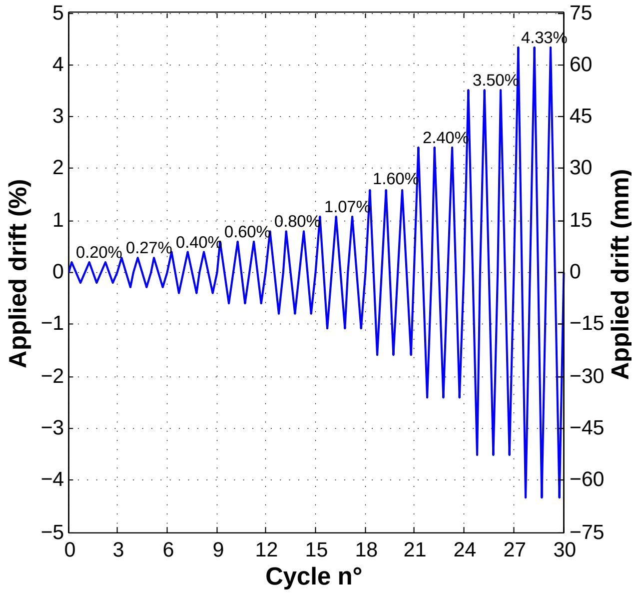

Figure 13: Test sequence of the displacement controlled cycles.

the 4.33% drift cycle. Thus, after having verified that the third complete cycle at drift ratio of 3.5% presented a peak force not less than 0.75 times the maximum applied force for the same direction, just one more drift ratio at 4.33% has been investigated.

Before going to the main experimental results it is helpful to understand how the vertical force applied on the top of the specimen varied during the experimental test for the imposed horizontal displacement. From Fig. 14 it can be noted that, starting from the initial value of 155 kN (scaled permanent axial load due to the overlying portion of the structure), the force increases as the imposed displacement increases. This behavior corresponds to that occurring in the real structure during an earthquake excitation.

The main findings on the behavior of the precast joint in comparison with that of the cast-in-situ joint can be drawn observing the force vs. drift

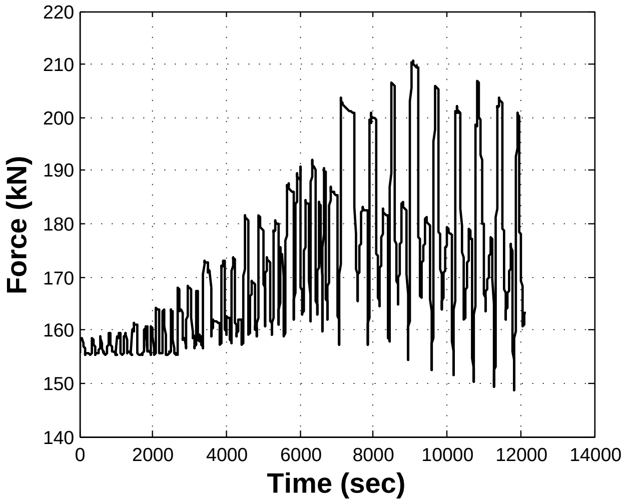

Figure 14: Time history of the axial force applied on the top of the specimen during the experimental test.

responses recorded during the two experimental tests, shown in Fig. 15. First of all, it can be noted that the drift-load relationship of the precast specimen is very similar to that obtained by other researchers for analogous connections [10, 31] with a stable ductile behavior for drift values in the range 1.5%-4.3%. The summary data of the the tests are listed in the Table 5. It is evident that the strength and the ductility of the two specimens are very similar. Indeed, the precast joint behavior (dashed lines) appears to be even more resistant than the cast-in-situ joint (solid lines) without appreciable changes to the ductility of the joint. In fact, the cast-in-situ specimen started yielding under positive drift values with an applied load of roughly 40 kN while the precast joint yielded as a result of the application of a 50 kN horizontal force. A similar observation with slightly higher force values can also be done for negative drift values. The first value is in very

Specimen	Positive displacement		Negative displacement	
	Max load (kN)	**Displ.** (mm)	**Max load** (kN)	**Displ.** (mm)
Cast-in-situ	50.0	51.0	-59.5	-51.2
Precast	58.1	59.3	-69.7	-61.4

Table 5: Summary of the test results.

good agreement with that resulting from the calculation in correspondence of the yielding of the beam steel rebars equal to 35.0 kN obtained as the ratio between the nominal bending strength $M_{n,red} = 47.2$ kNm and the distance $L/2 = 1.35$ m between the critical section and the beam support. The second one is higher than that expected for the higher compressive strength of the FRC.

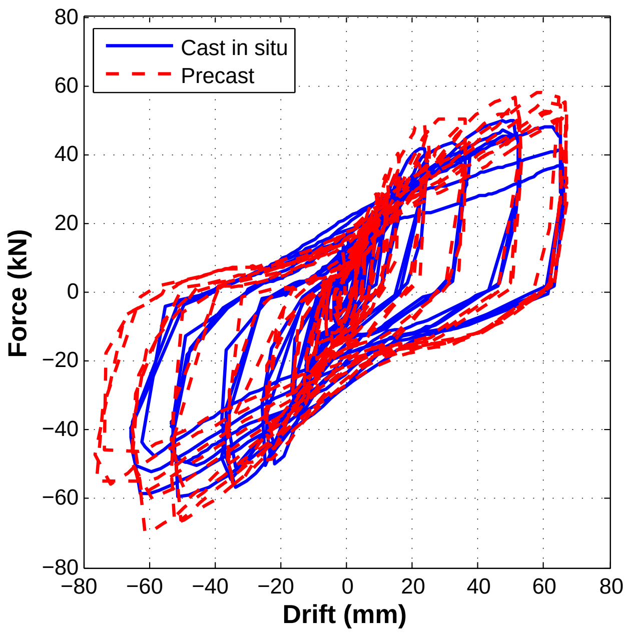

Figure 15: Force vs drift response of the cast-in-situ (solid curve) and the precast (dashed curve) specimens.

The crack patterns observed at the end of the tests for the cast-in-situ and the precast joints are shown in Fig. 16. The cracking pattern inside the joint region for both cases was similar to that obtained for this type of exterior beam-column connections by other researchers [32, 33, 10]. In particular, cracks with an inclination of roughly ±45°on the horizontal have been detected inside the joint region while horizontal cracks have been detected just above and just below the joint region. For the monolithic connection a diffused cracking is present in the critical zone of the beam with very few cracks in the column. A main crack, located in the beam at about 100 mm from the column face, is also visible in the picture. A severe concrete spalling also occurred in the top concrete cover. The precast connection shows an apparent reduced state of cracking in the critical zone but also in this case a main crack, located at roughly 50 mm from the column face, occurred during the tests. Nevertheless, the real state of the cracking occurred in the FRC matrix is not visible since it is hidden by the lateral precast concrete plates used as formworks. The presence of the crack at the beam-column connection can be inferred by looking at Fig. 18b and in particular to the data recorded by the sensors LVDTH1 and LVDTH2. In fact it can be noted that the readings of these sensors are not symmetric with positive values (lengthening) much greater than the negative ones (shortening). The difference between these two values is representative of the main crack amplitude.

The sensors embedded in the specimens allowed to carry out an in-depth analysis of the stress state in the materials. Among the available data, the most interesting ones turned out to be those provided by the VWSG connected to the upper rebars. These data are shown in Fig. 17. The strains

(a)

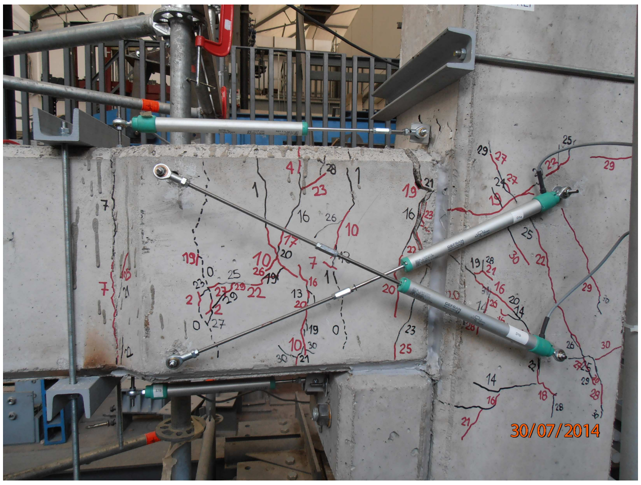

(b)

Figure 16: Crack patterns at the end of the tests for: (a) the cast-in-situ and (b) the precast joints.

recorded by the sensors placed inside the cast-in-situ and the precast beams gradually increased up to a drift ratio of 2.4% corresponding to a top displacement of ±36 mm. Afterward the steel strain has maintained maximum deformation values practically constant up to the end of the tests. This behavior can be ascribed to the yielding of the reinforcing bars within the critical zone. Nevertheless it should be emphasized that the maximum strain value recorded in the cast-in-situ joint is slightly higher (approx 2250 $\mu\epsilon$) than that observed in the precast joint (approx 1750 $\mu\epsilon$). Most likely this occurred for the overlapping of the rebars in the precast specimen that prevented the yielding of the rebars in the area where they are fully overlapped and caused the yielding of the steel rebars just outside this area. A confirmation to this thesis has been obtained observing the data gathered from the VWSG placed inside the column, also plotted in the same figure. Values well above the yielding deformation, shown in the Table 3, have been in fact recorded by this sensor. For the precast specimen it can thus be noted that the zone where the yielding of the steel rebars take place is just between the end of the loop coming from the beam and the lateral side of the column, as confirmed by the above mentioned crack pattern. This finding also demonstrates the ability of the proposed connection system to transmit the bending moment to the column. Nevertheless, the yielding of the steel rebars can produce tensile cracks inside the column resulting in a not negligible damage of concrete. The use of protruding reinforcing bars with diameter larger than those of the connected beam would avoid this excessive concrete damage inside the joint, inducing the steel yielding to occur only inside the beam as will be shown in the next section by means of FE analysis.

The influence of the shear deformation on the total deformation of the beam critical region can be observed by looking at the data recorded by the

PDTs during the experimental tests shown in Fig. 18. The mean transversal displacement of the section placed at 360 mm from the column face can be obtained by using trigonometry equations reported in the enclosed Appendix. This value is made up of the flexural and the shear deformation of the beam critical zone. The contribution of the shear deformation can be extracted from the data recorded by the PDTs according to the method proposed by Massone and Wallace [34]. From the comparison of the two values shown in Fig. 19 it can be deduced that the shear deformation is negligible in the elastic range and for small amount of the damage in the specimens. The effect produced by the occurrence of the main crack is, instead, relevant as can be deduced by comparing the graphs of Figs. 18 and 19. It can be, in fact, observed that at the same time at which the elongation recorded by LVDTs starts increasing rapidly (due to the formation of the main crack) the shear deformation also starts increasing. This happens after roughly 5800 sec for the cast-in-situ specimen (Fig. 18a and Fig. 19a) and around 4600 sec for the precast specimen (Fig. 18b and Fig. 19b). It can, thus, be deduced that the severe cracking reduced in a consistent way the shear stiffness of the joint.

To summarize, the progressive damage and collapse observed in the two types of joint can be judged very similar with the only difference that in the cast-in-situ joint the spalling of the upper concrete cover, probably due to the lower concrete strength and to the absence of the steel fibers with respect to FRC, prevented the attainment of higher lateral forces.

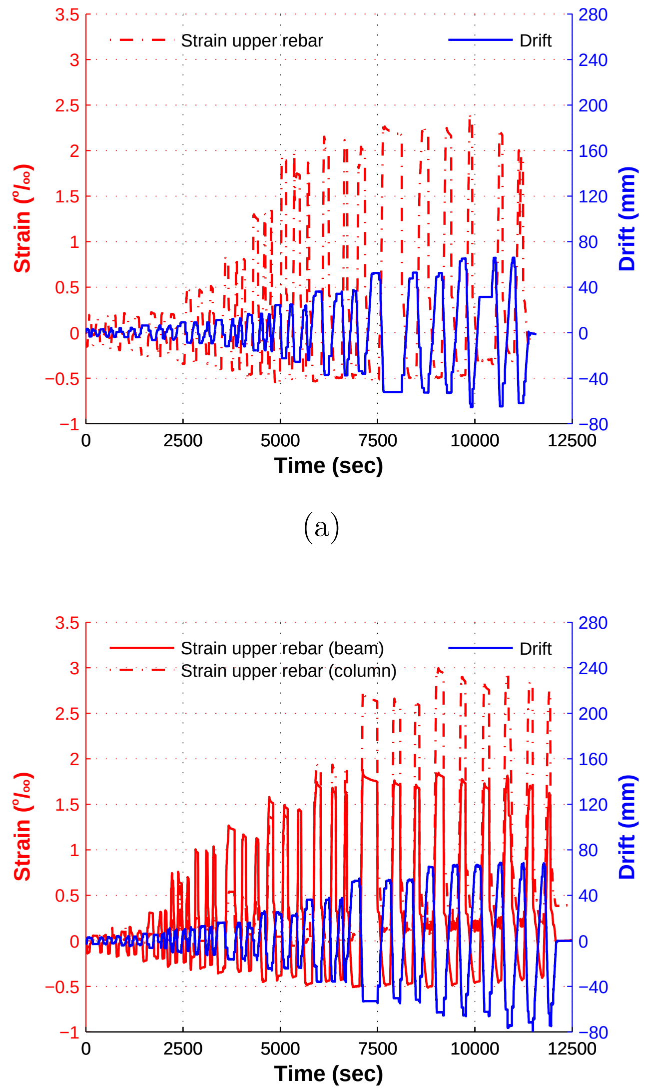

(a)

(b)

Figure 17: Strains recorded in the upper rebars: (a) in the cast-in-situ and (b) in the precast joints.

6. Improvement of the connection system

The experimental tests carried out on the precast specimen allowed to validate the connection system between the beam and the pillar demonstrat-

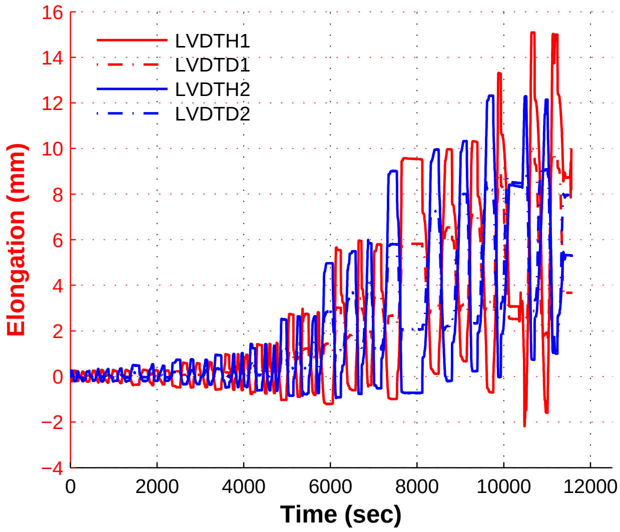

(a)

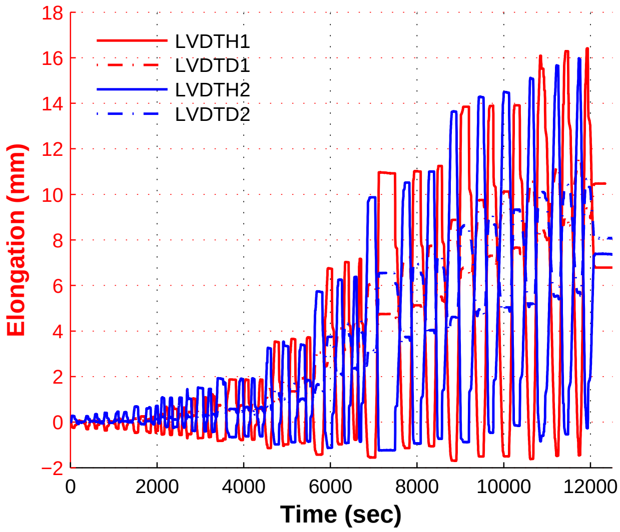

(b)

Figure 18: Elongation recorded by the LVDTs: (a) in the cast-in-situ and (b) in the precast joints.

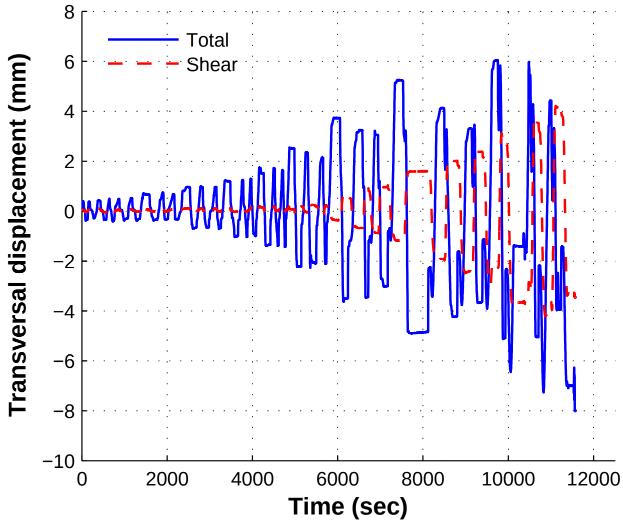

(a)

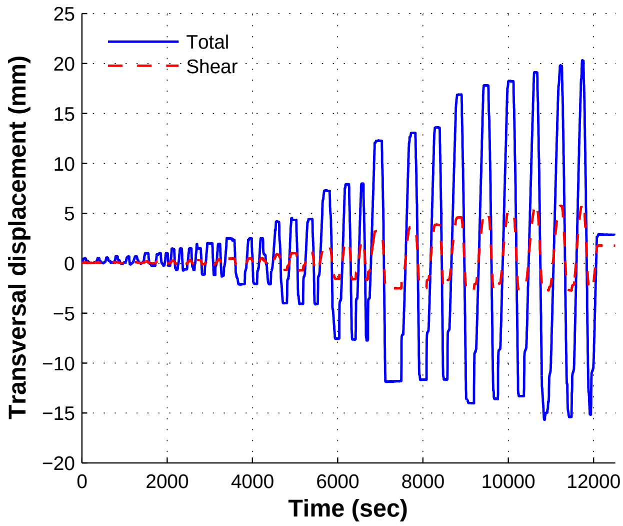

(b)

Figure 19: Total (solid line) and shear (dashed line) transversal deformation: (a) in the cast-in-situ and (b) in the precast joints.

ing that the prefabricated solution has a behavior quite similar, if not better, than that of the cast-in-situ solution. Nevertheless, the measurements carried out with the VWSGs connected to the reinforcing bars of the beam showed a significant steel yielding in correspondence of the rebars portion in the joint inside the column. As a consequence, a not negligible concrete cracking inside the column (see Fig. 16b) was produced, a type of damage that should generally be avoided.

The connection system between the precast beam and column easily allow to overcome this drawback by simply adopting protruding bars from the beam having a smaller diameter than those protruding from the column. This modification will cause the shift of the steel yielding zone inside the beam, just outside the area of overlap of the rebars (section with M_{Rd2} in Fig. 20). In fact, the presence of overlapping rebars neglect the steel yielding in this area. The reduction in the bar diameter depends on the extent of the overlapping length l_1 and can be estimated by the following equation:

$$\gamma_{Rd} \cdot M_{Rd2} \leq M_{Rd1} \cdot \frac{L - 2l_1}{L} - \Delta M_{Ed,1,2} \qquad (1)$$

where M_{Rd1} and M_{Rd2} are the resisting moments of the sections just outside the column and just outside the overlapping area, L is the length of the beam, γ_{Rd} is an overstrength factor to take into account the uncertainty on the resistances design values in the estimation of the capacity design action effects, as done for instance by EN 1998 [35] and $\Delta M_{Ed,1,2}$ is the difference between the bending moment in the sections 1 and 2 (see Fig. 20) produced by the vertical loads. Moreover, the following design controls must be carried out to ensure a correct hierarchy of resistances avoiding brittle shear failures in the beam:

$$V_{Rd1} \geq (g + \psi_2 q) \cdot \frac{L}{2} + \gamma_{Rd} \cdot \frac{2M_{Rd1}}{L} \tag{2}$$

$$V_{Rd2} \geq (g + \psi_2 q) \cdot \frac{L - 2l_1}{2} + \gamma_{Rd} \cdot \frac{2M_{Rd2}}{L - 2l_1} \tag{3}$$

where V_{Rd1} and V_{Rd2} are the shear strength of the sections just outside the column and just outside the overlapping area, g is the self weight load and $\psi_2 q$ is the variable load acting on the beam in the seismic load combination.

To avoid failure inside the beam-column joint it must be also checked that the diagonal compression force induced in the joint by the diagonal strut mechanism does not exceed the compressive strength of the concrete. For instance, EN 1998 [35] assumes satisfied this clause for exterior beam-column joints if the following inequality holds:

$$V_{jRd} \geq V_{jEd} \tag{4}$$

having indicated with

$$V_{jRd} = 0.8\eta \cdot f_{cd} \sqrt{1 - \frac{\nu_d}{\eta}} \cdot b_j \cdot h_{jc} \tag{5}$$

where $\eta = 0.6(1 - f_{ck}/250)$, h_{jc} is the distance between the extreme layers of column reinforcement, b_j is the effective joint width, ν_d is the normalized axial force in the column above the joint, f_{ck} is the concrete characteristic strength given in MPa and with V_{jEd} the maximum horizontal shear that can act on the core of the joint. This latter can be calculate for an exterior beam-column joint as follow:

$$V_{jEd} = \gamma_{Rd} \cdot A_{s1} \cdot f_{yd} - V_C \tag{6}$$

with A_{s1} the area of the beam top reinforcement, V_C the shear force in the column above the joint and γ_{Rd} the already mentioned factor to account for steel overstrength.

For instance, for the precast joint tested in this work Eq. 4 turned out to be:

$$V_{jEd} = 248.4kN < 355.7kN = V_{jRd} \tag{7}$$

having assumed $\gamma_{Rd} = 1.20$, $A_{s1} = 380mm^2$, $f_{yd} = 391.3MPa$, $V_C = -70kN$, $f_{ck} = MPa$, $b_j = 167mm$, $h_j = 250mm$, $N_c = 210kN$.

Finally, the column has to be over-designed with respect to the beam flexural strength M_{Rd1}. At the same time, the dimension of the FRC cast has been shortened from 323 mm to 214 mm to reduce the construction costs and to simplify the building. By doing so, the width of the joint became smaller than that recommended by the relevant *fib* standard [24] for loop connections in wet joints with conventional concretes. However, it has already been shown that this reduction can be achieved by using FRC [36]. According to Eq. 1 this reduction also allows to increase the bending strength M_{Rd2} that should be provided by the rebars protruding from the beam. Finally, the beam longitudinal steel reinforcement of the original joint (2 ϕ 12 mm and 1 ϕ 14 mm rebars, see Fig. 6) has been reduced based on the same equation to 2 ϕ 12 mm and 1 ϕ 10 mm rebars.

Nevertheless, the overlapping can not be too small to provide a suitable force transfer, even if each bar has an hook shape and can thus be considered as self-anchored. The improvement of the structural behavior achievable with this solution has been tested by means of nonlinear finite element analysis described in the following paragraphs.

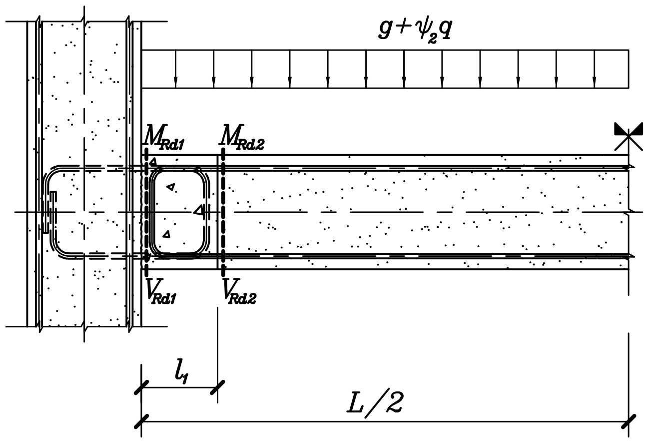

Figure 20: Geometrical dimensions and reference bending and shear strengths of the precast beam.

6.1. Numerical models

Two different models, shown in Fig. 21, have been implemented with the general purpose commercial finite element software ABAQUS for the tested specimen and for the modified configuration. 8-node brick finite elements have been used to model the concretes while the reinforcement bars were modeled by 2-noded truss elements.

The mechanical model adopted for the concrete is the "Concrete Damaged Plasticity" (CDP). This model is suitable for analyzing the inelastic behavior of concrete under monotonic, cyclic or dynamic loading. It also allows evaluating the degradation of material stiffness during cyclic loadings by means of damage parameters. The main parameters defined to model the concrete behaviour were density, tangent elastic stiffness and CDP model parameters. Among these latter the most important ones were the two stress-strain inelastic constitutive laws for concrete subject respectively to monotonic tension and compression. Additional parameters specified for the CDP model are dilation angle Ψ, eccentricity ε, ratio σ_{b0}/σ_{c0} between the initial equibiaxial compressive yield stress to initial uniaxial compressive yield stress and parameter K_c (ratio of the second stress invariant on the tensile meridian to that on the compressive meridian). These latter parameters have been assumed equal to the reference values for typical concretes [37]. Their values are given in Table 6. No viscoplastic regularization has been implemented in the model as well as no compressive and tensile damage variables were specified since no cyclic loading has been imposed to the concrete.

The compression non-linear stress-strain curves proposed by the *fib* Model Code 2010 [38] have been used for both the concrete of the precast elements and for the FRC:

$$\sigma_c = f_{cm} \cdot \frac{k \cdot \eta - \eta^2}{1 + (k - 2) \cdot \eta} \tag{8}$$

where $\eta = \epsilon_c/\epsilon_{c1}$, $k = E_{ci}/E_{c1}$, ϵ_c is the concrete strain, ϵ_{c1} is the strain at maximum compressive stress, E_{ci} is the modulus of elasticity at concrete age of 28 days, E_{c1} is the secant modulus from the origin to the peak compressive stress and k is the plasticity number provided by the Model Code. For the tensile non-linear stress-strain curve of the FRC, based on the data found in the literature [39] and considering the low volume fraction of the steel fibers, a strain-softening behaviour has been assumed for the FRC. The tensile strain softening curves shown in Fig. 22(a) have been deduced from the experimental tests carried out on similar concretes by Yang et al. [40].

The steel reinforcements have been modeled using an elasto-plastic constitutive law with strain hardening. The stress-strain relationships for these materials are shown in Fig. 22(b).

The interaction between rebars and concrete has been implemented by modeling the reinforcements as embedded elements hosted in the concrete solid parts. This constraint eliminates the degrees of freedom of the rebar mesh nodes and forces these latter to displace by interpolating the neighbouring concrete mesh nodal displacements. Low friction and weak adhesion has been used to simulate the contact between the two type of concretes. An increasing displacement has been imposed to the top of the RC column and suitable boundary conditions have been applied to simulate the experimental test. For the purpose of this analysis the cumulative damage provided by the cyclic loading has been neglected.

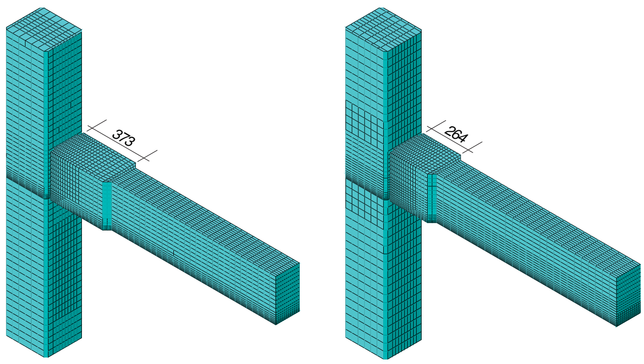

Figure 21: FE models of the original precast joint (left) and of the modified precast joint (right) with dimensions of connection zone in mm.

6.2. *Results of the FE simulations*

The results of the FE simulations can be summarized by considering the relationship between the force applied to the RC column and its displacement. It must be first observed that a quite good agreement has been obtained between the curve of the experimental tests and that of the equivalent FE model, as observable in Fig. 23, thus validating the numerical

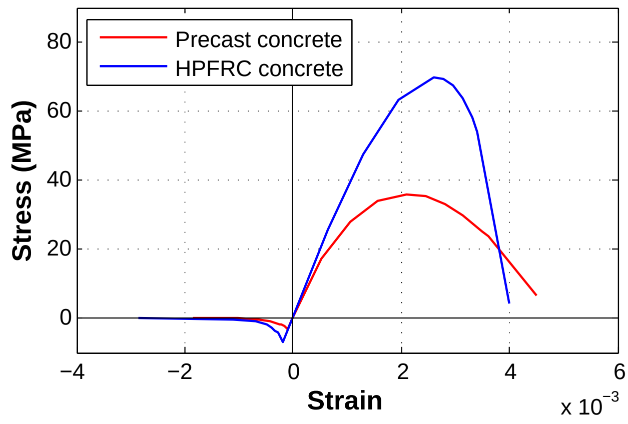

(a)

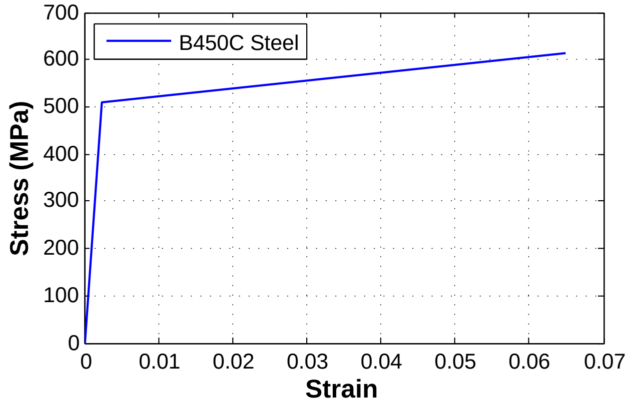

(b)

Figure 22: Stress-strain relationships for: (a) the concretes and (b) the reinforcing steel.

model. In the same figure is also shown the force-displacement curve for the joint with the modified configuration. It can be noticed that the behavior is very similar to that of the original configuration. The improvements of the structural behavior are, however, visible in Fig. 24 where is represented the stress state of the rebars in the two configurations. As visible, in the original

Material parameters		
Parameter	Precast concrete	FRC
ρ (Kg/m^3)	2300	2300
E_0 (MPa)	32308	39441
ν	0.1	0.1
ε	0.1	0.1
Ψ	35°	35°
K_c	2/3	2/3
σ_{b0}/σ_{c0}	1.16	1.16
σ_{cu} (MPa)	36	70
ϵ_u	0.0045	0.004
σ_{tu} (MPa)	3.32	7
d_c	0	0
d_t	0	0
w_c	0	0
w_t	0	0

Table 6: Assumed values for the CDP parameters of the precast concrete and FRC.

configuration the yielding of the rebars, indicated with red color, takes place primarily within the node in the pillar while it moved into the beam outside the area of overlapping in the modified configuration. The persistence in the elastic range of the reinforcing bars embedded in the pillar and the presence of damage only inside the beam also allows for the realization of easier repairs in the case of severe earthquakes. Nevertheless, it has to be highlighted that the shortening of the splice length produces an increase in the compression principal stresses in the FRC inside the overlapping region. In fact the maximum concrete compressive stress inside the loop splice is approximately equal to 8 MPa in the original precast joint, as shown in Fig. 25, and becomes roughly 13 MPa in the modified precast joint. Whereas this value is still acceptable for the mechanical properties of the FRC, further experimental investigations should be performed for real design cases.

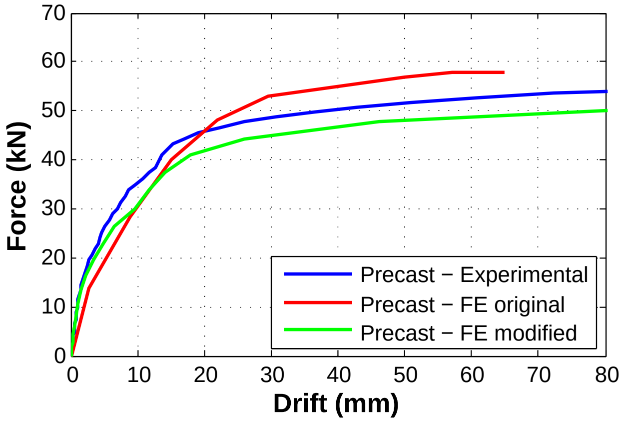

Figure 23: Comparison between the experimental force-displacement envelope and the force-displacement curves of the two FE models.

7. Conclusions

A technique to realize beam-column joints in precast RC frames has been presented in this paper. It is based on prefabricated beams and columns with protruding bars that are connected in-situ by means of a concrete wet joint with steel fibers to moderately increase the ductility properties of the compressed struts in the joint. Experimental tests allowed comparing the structural behavior of a beam-column sub-assemblage realized with this technique to that of an equivalent cast-in-situ beam-column joint. The results of these tests showed that the two solutions exhibited very similar structural behaviors, with the proposed solution achieving a slightly greater strength and stiffness than those of the cast-in-situ solution without relevant modifications to the joint ductility. Numerical simulations have been subsequently performed to improve the damaging mechanism of the precast beam-column connection. In detail, the arrangement of the reinforcing steel has been up-

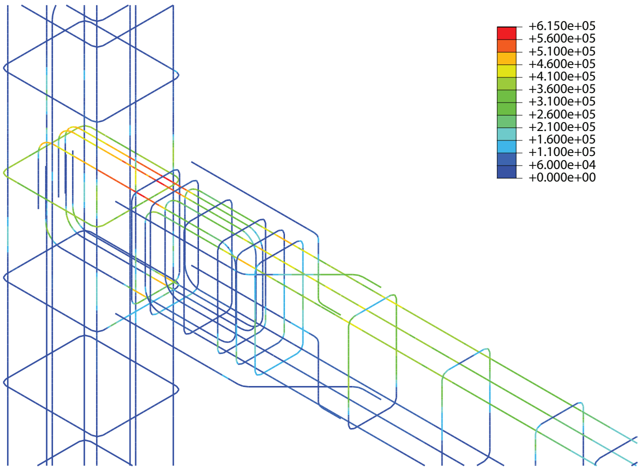

(a)

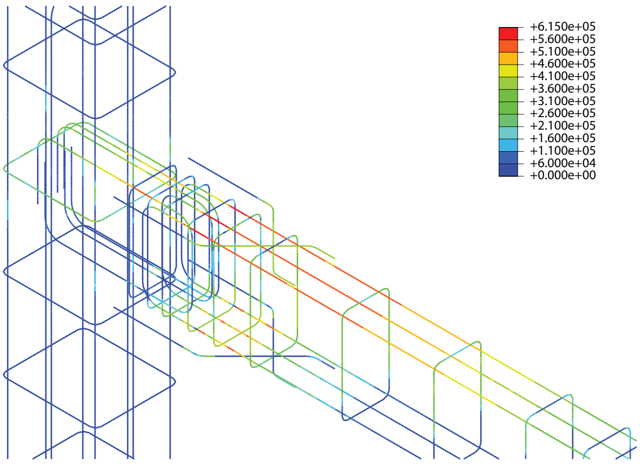

(b)

Figure 24: Stress state of the rebars in the FE models: (a) original precast joint and (b) modified precast joint. Yielded rebars are shown in red. Values in kPa.

dated in order to avoid the yielding of the steel inside the column and to move the plastic zone inside the beam. The so-obtained damage pattern has been thus concentrated in the beam, allowing for easier restoration works

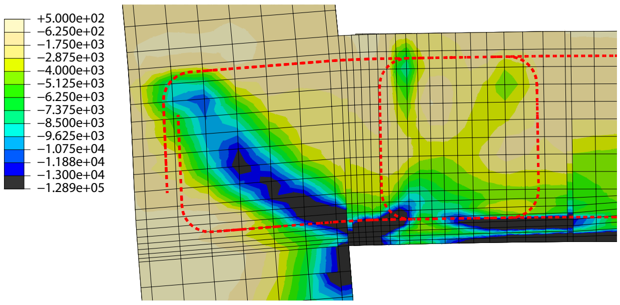

(a)

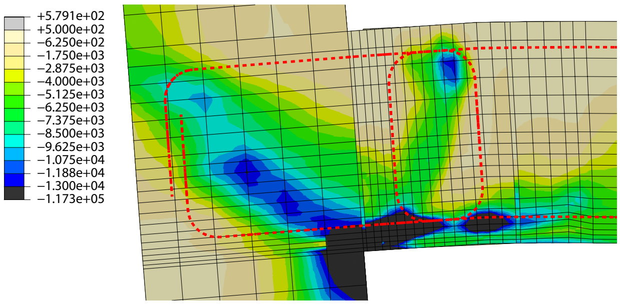

(b)

Figure 25: Minimum principal stresses in the FE models: (a) original precast joint and (b) modified precast joint (Values in kPa, Loop splices indicated with dashed lines).

that should be carried out after a severe earthquake.

Acknowledgments

This research was supported by the jointventure ETILENO XXI Contractors SAPI de CV between the firms Technip, Odebrecht and Icafluor. The authors would like to extend their sincere thank to Mr Ascenzo Burzichelli and Mr Paolo Lopriore, respectively Project Director and Head of Engineering Department at Technip Italy s.p.a., for their invaluable assistance.

Appendix

With the symbols shown in Fig. 26, the following angles have been calculated:

$$\alpha_1 = \arccos\left[\frac{(b_1+\Delta b_1)^2 + c^2 - (d_1+\Delta d_1)^2}{2c\,(b_1+\Delta b_1)}\right] \tag{9}$$

$$\alpha_2 = \arccos\left[\frac{(b_2+\Delta b_2)^2 + c^2 - (d_2+\Delta d_2)^2}{2c\,(b_2+\Delta b_2)}\right] \tag{10}$$

where b_1, b_2, c, d_1 and d_2 are the dimension of the initial LVDT configuration and Δb_1, Δb_2, Δd_1 and Δd_2 are the readings of the LVDT during the tests. Referring to the coordinate system of the above mentioned figure, the transversal coordinates of points 1 and 2 can be calculated as:

$$y_1 = \frac{c}{2} - (b_1+\Delta b_1)\cdot cos\,(\alpha_1) \tag{11}$$

$$y_2 = -\frac{c}{2} + (b_2+\Delta b_2)\cdot cos\,(\alpha_2) \tag{12}$$

The transversal displacement of the mean point of segment $\overline{12}$ is thus equal to:

$$y_m = \frac{y_1+y_2}{2} \tag{13}$$

According to Massone and Wallace [34] and assuming small deformations inside the node region the shear displacement can be calculated as follows:

$$y_{m,s} = \frac{\sqrt{(d_1+\Delta d_1)^2 - c^2} - \sqrt{(d_2+\Delta d_2)^2 - c^2}}{2} + \\ + \left(\frac{1}{2} - \alpha\right)\cdot l \cdot \cos\left(\frac{\alpha_1 + 180 - \alpha_2}{2}\right) \tag{14}$$

with α equal to 0.67.

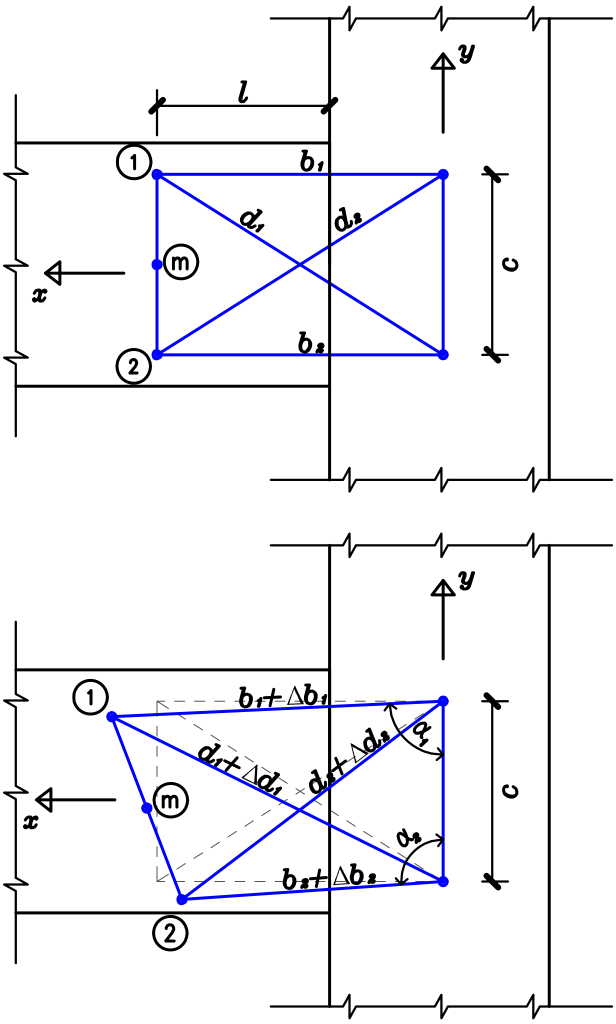

Figure 26: LVDT lengths in the initial (top) and deformed (bottom) configurations.

References

[1] T. Paulay, R. Park, M. Priestley, Reinforced concrete beam-column joints under seismic actions., J Am Concr Inst 75 (11) (1978) 585–593.

[2] T. Paulay, Equilibrium criteria for reinforced concrete beam-column

joints, ACI Structural Journal 86 (6) (1989) 635–643.

[3] M. Priestley, Overview of presss research program, PCI Journal 36 (4) (1991) 50–57.

[4] M. Priestley, S. Sritharan, J. Conley, S. Pampanin, Preliminary results and conclusions from the presss five-story precast concrete test building, PCI Journal 44 (6) (1999) 42–67.

[5] J. I. Restrepo, R. Park, A. H. Buchanan, Test on connections of earthquake resisting precast reinforced concrete perimeter frames of buildings, PCI Journal 40 (4) (1995) 44–61.

[6] M. Priestley, G. MacRae, Seismic tests of precast beam-to-column joint subassemblages with unbonded tendons, PCI Journal 41 (1) (1996) 64–80.

[7] S. Alcocer, R. Carranza, D. Perez-Navarrete, R. Martinez, Seismic tests of beam-to-column connections in a precast concrete frame, PCI Journal 47 (3) (2002) 70–89.

[8] H. H. Korkmaz, T. Tankut, Performance of a precast concrete beam-to-beam connection subject to reversed cyclic loading, Engineering Structures 27 (9) (2005) 1392 – 1407.

[9] K. Ong, Z. S. Lin, L. R. Chandra, C. T. Tam, S. D. Pang, Experimental investigation of a DfD moment-resisting beamcolumn connection, Engineering Structures 56 (0) (2013) 1676 – 1683.

[10] H. Parastesh, I. Hajirasouliha, R. Ramezani, A new ductile moment-resisting connection for precast concrete frames in seismic regions: An experimental investigation, Engineering Structures 70 (0) (2014) 144 – 157.

[11] P. Negro, D. Bournas, F. Molina, Pseudodynamic tests on a full-scale 3-storey precast concrete building: Global response, Engineering Structures 57 (2013) 594–608.

[12] D. Bournas, P. Negro, F. Molina, Pseudodynamic tests on a full-scale 3-storey precast concrete building: Behavior of the mechanical connections and floor diaphragms, Engineering Structures 57 (2013) 609–627.

[13] R. Vidjeapriya, K. Jaya, Experimental study on two simple mechanical precast beam-column connections under reverse cyclic loading, Journal of Performance of Constructed Facilities 27 (4) (2013) 402–414.

[14] H.-K. Choi, Y.-C. Choi, C.-S. Choi, Development and testing of precast concrete beam-to-column connections, Engineering Structures 56 (0) (2013) 1820 – 1835.

[15] G. Cheok, W. Stone, S. Kunnath, Seismic response of precast concrete frames with hybrid connections, ACI Structural Journal 95 (5) (1998) 527–538.

[16] K. Ong, J. Hao, P. Paramasivam, A strut-and-tie model for ultimate loads of precast concrete joints with loop connections in tension, Construction and Building Materials 20 (3) (2006) 169 – 176.

[17] H.-K. Ryu, Y.-J. Kim, S.-P. Chang, Experimental study on static and fatigue strength of loop joints, Engineering Structures 29 (2) (2007) 145 – 162.

[18] H. B. Joergensen, L. C. Hoang, Tests and limit analysis of loop connections between precast concrete elements loaded in tension, Engineering Structures 52 (2013) 558 – 569.

[19] A. E. Naaman, J. K. Wight, H. Abdou, SIFCON connections for seismic resistant frames, Concrete International 9 (11) (1987) 34–39.

[20] R. Vasconez, A. Naaman, J. Wight, Behavior of HPFRC connections for precast concrete frames under reversed cyclic loading, PCI Journal 43 (6) (1998) 58–71.

[21] L. Maya, C. Zanuy, L. Albajar, C. Lopez, J. Portabella, Experimental assessment of connections for precast concrete frames using ultra high performance fibre reinforced concrete, Construction and Building Materials 48 (2013) 173 – 186.

[22] *ACI* Committee 318, Building Code Requirements for Structural Concrete (ACI 318-08) and Commentary, ACI, Farmington Hills, MI (2008).

[23] A. Bruggeling, G. Huyghe, Prefabrication with concrete, Balkema, Rotterdam, 1991.

[24] *fib* International Federation for Structural Concrete Task Group 6.2, Bulletin 43 - Structural connections for precast concrete buildings, *fib*, Lausanne (2008).

[25] *ACI* Innovation Task Group 1, Acceptance Criteria for Moment Frames Based on Structural Testing (ACI T1.1-01), ACI, Farmington Hills, MI (2001).

[26] *ACI* Innovation Task Group 1, Commentary on Acceptance Criteria for Moment Frames Based on Structural Testing (ACI T1.1R-01), ACI, Farmington Hills, MI (2001).

[27] L. Taerwe, A. Van Gysel, Influence of steel fibers on design stress-strain curve for high-strength concrete, Journal of Engineering Mechanics 122 (8) (1996) 695–704.

[28] R. Neves, J. De Fernandes Almeida, Compressive behaviour of steel fibre reinforced concrete, Structural Concrete 6 (1) (2005) 1–8.

[29] K. Marar, O. Eren, I. Yitmena, Compression specific toughness of normal strength steel fiber reinforced concrete (nssfrc) and high strength steel fiber reinforced concrete (hssfrc), Materials Research 14 (2) (2011) 239–247.

[30] *ACI* Committee 544, State-of-the-Art Report on Fiber Reinforced Concrete (ACI 544.1R-96), ACI, Farmington Hills, MI (1996).

[31] H.-J. Im, H.-G. Park, T.-S. Eom, Cyclic loading test for reinforced-concrete-emulated beam-column connection of precast concrete moment frame, ACI Structural Journal 110 (1) (2013) 115–125.

[32] O. Ertas, S. Ozden, T. Ozturan, Ductile connections in precast concrete moment resisting frames, PCI Journal 51 (3) (2006) 66–76.

[33] A. Tsonos, Cyclic load behavior of reinforced concrete beam-column subassemblages of modern structures, ACI Structural Journal 104 (4) (2007) 468–478.

[34] L. Massone, J. Wallace, Load-deformation responses of slender reinforced concrete walls, ACI Structural Journal 101 (1) (2004) 103–113.

[35] CEN, EN 1998-1 - Eurocode 8: Design of structures for earthquake resistance - Part 1: General rules, seismic actions and rules for buildingsg, CEN European Committee for Standardization, Brussels, B (2004).

[36] D. de Lima Arajo, M. C. Curado, P. F. Rodrigues, Loop connection with fibre-reinforced precast concrete components in tension, Engineering Structures 72 (2014) 140 – 151.

[37] D. Hibbitt, B. Karlsson, P. Sorensen, Abaqus Analysis User's Manual, Abaqus, Inc.

[38] *fib* International Federation for Structural Concrete, Model Code 2010, *fib*, Lausanne (2010).

[39] K. Wille, D. Kim, A. Naaman, Strain-hardening UHP-FRC with low fiber contents, Materials and Structures 44 (2011) 583–598.

[40] M. Yang, C. Huang, J. Wang, Characteristics of stress-strain curve of high strength steel fiber reinforced concrete under uniaxial tension, Journal of Wuhan University of Technology-Mater. Sci. Ed. 21 (3) (2006) 132–137.